LIMNOLOGY and OCEANOGRAPHY

ASLO

Limnol. Oceanogr. 65, 2020, 2866–2882

doi: 10.1002/lno.11558

Physical drivers facilitating a toxigenic cyanobacterial bloom in a major Great Lakes tributary

Paul G. Matson [1,a] Gregory L. Boyer,[2] Thomas B. Bridgeman,[3] George S. Bullerjahn,[1] Douglas D. Kane,[4,b] Robert M. L. McKay,[1,5] Katelyn M. McKindles,[1] Heather A. Raymond,[6,c] Brenda K. Snyder,[3] Richard P. Stumpf,[7] Timothy W. Davis[1]*

[1]Department of Biological Sciences, Bowling Green State University, Bowling Green, Ohio
[2]Department of Chemistry, State University of New York–College of Environment Science and Forestry, Syracuse, New York
[3]Lake Erie Center and Department of Environmental Sciences, University of Toledo, Toledo, Ohio
[4]Division of Natural Science, Applied Science, and Mathematics, Defiance College, Defiance, Ohio
[5]Great Lakes Institute for Environmental Research, University of Windsor, Windsor, Ontario, Canada
[6]Division of Drinking and Ground Waters, Ohio Environmental Protection Agency, Columbus, Ohio
[7]National Oceanic and Atmospheric Administration, National Centers for Coastal Ocean Science, Silver Spring, Maryland

Abstract

The Maumee River is the primary source for nutrients fueling seasonal *Microcystis*-dominated blooms in western Lake Erie's open waters though such blooms in the river are infrequent. The river also serves as source water for multiple public water systems and a large food services facility in northwest Ohio. On 20 September 2017, an unprecedented bloom was reported in the Maumee River estuary within the Toledo metropolitan area, which triggered a recreational water advisory. Here we (1) explore physical drivers likely contributing to the bloom's occurrence, and (2) describe the toxin concentration and bacterioplankton taxonomic composition. A historical analysis using 10-years of seasonal river discharge, water level, and local wind data identified two instances when high-retention conditions occurred over ≥ 10 d in the Maumee River estuary: in 2016 and during the 2017 bloom. Observation by remote sensing imagery supported the advection of cyanobacterial cells into the estuary from the lake during 2017 and the lack of an estuary bloom in 2016 due to a weak cyanobacterial bloom in the lake. A rapid-response survey during the 2017 bloom determined levels of the cyanotoxins, specifically microcystins, in excess of recreational contact limits at sites within the lower 20 km of the river while amplicon sequencing found these sites were dominated by *Microcystis*. These results highlight the need to broaden our understanding of physical drivers of cyanobacterial blooms within the interface between riverine and lacustrine systems, particularly as such blooms are expected to become more prominent in response to a changing climate.

Cyanobacterial harmful algal blooms (CHABs) have become a common seasonal occurrence in the western basin of Lake Erie and its embayments (Bullerjahn et al. 2016). Whereas the Maumee River and its watershed serve as an important source for the nutrients that fuel these blooms (Baker et al. 2014; Kane et al. 2014), CHABs in the river are sparsely documented (Bridgeman et al. 2012; Conroy et al. 2014; McKay et al. 2018). Further, when cyanobacterial blooms have been documented in the river, they have occurred in spring or early summer with late summer blooms being less common (Bridgeman et al. 2012; Conroy et al. 2014; McKay et al. 2018).

The Maumee River drains into Lake Erie, forming a freshwater estuary that is influenced by riverine and lacustrine processes within the Toledo (OH) metropolitan area (Herdendorf 1970). On 20 September 2017, reports emerged of a CHAB developing within the Maumee River estuary, prompting the Toledo-Lucas County Health Department to issue a recreational public health advisory to avoid contact. The Maumee River serves as source water for multiple Ohio public water systems including the communities of Napoleon, Bowling Green, and Defiance as well as

*Correspondence: timdavi@bgsu.edu

Additional Supporting Information may be found in the online version of this article.

[a]Present address: Environmental Sciences Division, Oak Ridge National Laboratory, Oak Ridge, Tennessee, USA
[b]Present address: Biology and Environmental Sciences Department and National Center for Water Quality Research, Heidelberg University, Tiffin, Ohio, USA
[c]Present address: College of Food, Agriculture, and Environmental Sciences, The Ohio State University, Columbus, Ohio, USA

the Campbell Soup Company (Napoleon, OH). Incident-response cyanotoxin sampling began at Ohio public water systems in 2010, but routine water quality monitoring of the Maumee River was not conducted until HAB monitoring rules were enacted in 2016. Most university research efforts have been focused on the open waters of Lake Erie. As a result, fewer data are available from the Maumee River and estuary on cyanobacterial bloom composition, toxin concentrations or potential for organisms to produce toxins other than microcystins.

A diverse range of cyanobacteria capable of forming blooms are found within the western Lake Erie watershed. While *Microcystis* spp. is the common bloom-forming genus found in the lake (Conroy et al. 2005; Davis et al. 2014; Bullerjahn et al. 2016), riverine blooms are more commonly caused by *Planktothrix* spp. (Kutovaya et al. 2012; Davis et al. 2014; McKay et al. 2018). The presence of different taxa may influence the type of toxins produced, which may include microcystins, anatoxins, cylindrospermopsins, saxitoxins (PSTs), or the non-proteinogenic amino acid β-methylamino alanine (BMAA) (Esterhuizen and Downey 2008; Pearson et al. 2010). Further, due to the high levels of genomic diversity across cyanobacteria strains, taxa may be either toxigenic or non-toxigenic (Humbert et al. 2013; Kurmayer et al. 2015; Meyer et al. 2017) thus decoupling bloom toxin concentration from cyanobacterial biomass (O'Neil et al. 2012; McKay et al. 2018).

While many of the biological (e.g., zooplankton grazing, viral lysis, parasitic fungi, microbial interactions) and chemical (e.g., nitrogen, phosphorus, trace metal concentrations) factors in CHAB formation and decline have been studied (see Davis and Gobler 2016 and references therein), often less attention is paid to the physical factors such as riverine discharge, seiche intensity, and wind that can play important roles in formation. For example, in western lake Erie the advection of planktonic propagules that could initiate the bloom can originate from riverine or lacustrine sources, as well via wind-driven resuspension of cyanobacterial resting cells or cysts present in sediments (Bridgeman et al. 2012; Chaffin et al. 2014; Conroy et al. 2014; Kitchens et al. 2018). In addition to delivering nutrients, riverine discharge can influence light transmission, which can select for taxa based on their photosynthetic efficiency (Scheffer et al. 1997). Further, discharge rates coupled with seiche intensity can influence flushing and retention time within freshwater estuaries (Trebitz et al. 2002; Trebitz 2006), potentially allowing for enhanced growth in optimal environments by modifying water column stratification, light availability, and advection of cells (Mitrovic et al. 2011).

Here we present results (1) identifying physically drivers that are potentially responsible for the September 2017 bloom in the Maumee River estuary, and (2) describing the toxin concentrations and taxonomic compositions within the bloom and surrounding waters. Ten-years of observations of physical parameters (river discharge, seiche intensity, and wind) and remote sensing imagery from 2016 and 2017 were analyzed to identify potential physical drivers of the bloom related to water exchange in the Maumee River estuary. In situ samples collected from a rapid response survey along a 160-km stretch of the Maumee River and adjacent sites in western Lake Erie during the bloom event were analyzed to determine chlorophyll-estimated biomass, toxin presence and concentration, and the bacterioplankton taxonomic composition.

Methods

Historical analysis of physical drivers of transport

A historical analysis of physical drivers of transport in the Maumee River estuary from 2008 to 2017 was conducted to identify conditions relevant to blooms and their frequency of occurrence over the past decade. Data pertaining to the physical transport of water within the estuary (riverine discharge, seiche intensity, and local wind direction) were downloaded from collecting agency websites. Discharge observations (30-min interval) of the Maumee River at Waterville, OH (USGS Station 04193500) were obtained from the USGS National Water Information System (https://waterdata.usgs.gov). Wind and water level observations (six-min intervals) at the mouth of the Maumee River (NOAA Station THRO1) were obtained from the NOAA National Data Buoy Center (www.ndbc.noaa.gov). Seiche intensity was quantified by calculating the one-half daily sum of water level increments, which represents the height of the water column moved due to oscillation across all frequency modes (Trebitz 2006). Daily values were calculated as sums (seiche intensity), means (discharge), or proportions (wind) of hourly observations from a given day. The local wind direction metric was calculated as the daily proportion of hourly winds originating from the east (45 to 135° N) and does not account for wind speed. Winds from this directional range would have the greatest contribution to surface transport into the estuary given its west–east geographic orientation to the lake. Seasonal anomalies were calculated as the observed daily values subtracted by the mean of daily values (wind) or the back-transformed log means of daily values (discharge and seiche intensity) from June–September 2008–2017. Percentiles for each observed parameter were calculated from the 2008–2017 dataset using an empirical cumulative distribution function. All analyses were conducted using the R computing framework version 3.5.1 (R Core Team 2018).

Remote sensing

Ocean Land Color Imager (OLCI) from the Copernicus Sentinel-3 mission was used to assess the spatial structure of cyanobacterial blooms in the western basin of Lake Erie during two separate periods: 26 July–6 August 2016 and 11–26 September 2017. The OLCI data sets were processed to Rayleigh-corrected reflectance (R) using NASA's SeaWiFS Data Analysis System (SeaDAS) standard l2gen software ("rho_s" dimensionless product) within NOAA's Satellite Automated Processing System (SAPS). Images were mapped to UTM projection with 300 m pixels using nearest neighbor resampling. Each OLCI image was masked for land with the standard 250 m landmask distributed with SeaDAS and for clouds using the cloud albedo, excluding bright reflectance water that has strong spectral variation (high

reflectance in the near-infrared and green and low in the red and blue) to avoid masking intense blooms that would otherwise be flagged as clouds. Clouds were flagged using threshold algorithms, corrected for turbid water. The cyanobacteria detection algorithm used second derivative spectral shapes (SS) on the reflectance spectra with an equation:

$$SS(\lambda) = R(\lambda) - R(\lambda^-) + \{R(\lambda^-) - R(\lambda^+)\} \times \frac{(\lambda - \lambda^-)}{(\lambda^+ - \lambda^-)}$$

with λ = 681 nm, λ^+ = 709 nm, and λ^- = 665 nm (Wynne et al. 2010; Stumpf et al. 2016), and additional specificity for cyanobacteria by detecting the presence of phycocyanin uses shape with λ = 665 nm, λ^+ = 681 nm, and λ^- = 620 nm (Lunetta et al. 2015).

Study region and sample collection

Beginning on 25 September and continuing through 28 September, a total of 18 sites were sampled spanning the length of the Maumee River through Ohio from near the Indiana border (Fig. 1), though not all sample types were collected from every site (see below). The study area includes the shallower river sites (> 20 km upriver from Lake Erie, MR159–MR52), deeper sites in the Maumee River estuary (from river mouth to ~ 20 km upriver from Lake Erie, MR15–0, inset box), and sites located in western Lake Erie (WB1–WB8) in both nearshore and open water environments (> 3 m depths, as defined in Davis et al. 2019).

Integrated surface water was collected from selected sites (see Results) on 25, 26, and 28 September 2017 and processed by either passing through filters in the field (nucleic acids) or whole water samples were returned on ice to the lab for processing. For sampling of nucleic acids, 20–240 mL of surface water was passed through 0.22 μm Sterivex filters immediately after collection in the field and stored on dry ice. Two Sterivex filters were collected from MR0, one from a nearshore surface scum (MR0_A) and the other collected further from shore and outside of the scum (MR0_B). Samples for algal pigment (chlorophyll *a* [Chl *a*]) quantification and detection of total microcystins (extracellular and intracellular) and other cyanotoxins including anatoxins, cylindrospermopsins, saxitoxins (PSTs), and BMAA were collected whole, stored on ice, and transported back to Bowling Green State University or the University of Toledo Lake Erie Center for processing.

Identification and quantification of cyanotoxins

Cyanotoxins were identified and quantified from selected sites (see Results) on 25, 26, and 28 September 2017. Total microcystins (MC; expressed as microcystin-LR equivalents) were quantified from whole-water samples following the Ohio EPA Division of Environmental Services total (extracellular and intracellular) microcystins—ADDA protocol using an enzyme-linked immunosorbent assay (ELISA) kit (Microcystins/Nodularins [ADDA]; Abraxis) at UTLEC. Whole water samples (generally 250–500 mL) were also filtered (GF/F) for the detection of particulate anatoxins, saxitoxins (PSTs), cylindrospermopsins, and MC variants at State University of New York College of Environmental Science and Forestry (SUNY-ESF). Filters were extracted in 50% methanol using probe ultrasound, clarified by centrifugation at 14,000 × *g* and the MCs determined using an untargeted reverse phase chromatography coupled with single quadrupole mass spectroscopy (LC–MS) screening method. Toxins were separated using an ACE C18 column (3.0 × 150 mm, MacMod

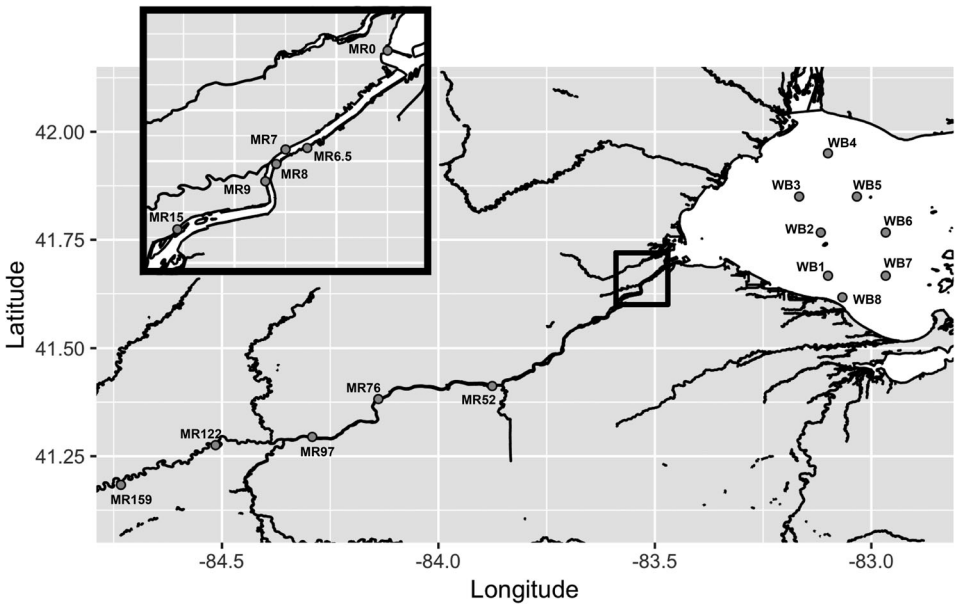

Fig. 1. Map of sampling sites (dark gray points) along Maumee River and in the western basin of Lake Erie. The inset box (black border) shows a larger-scale view of the Maumee River estuary sites in the Toledo Metro area.

Analytical, Chelmsford, PA) and a 30%–70% aqueous acetonitrile gradient containing 0.1% formic acid as the modifier (Boyer 2007). Individual toxins were identified on the basis of their retention time, their characteristic absorbance spectrum in the photodiode array detector, and their characteristic molecular ions. The LC–MS method described here used a Waters 2695 solvent delivery system coupled to a 2996 PDA detection and a ZQ4000 mass spectrometer (Waters Corporation, Milford MA). It specifically looks for the molecular ions (and/or their sodium adducts) of 22 common variants (RR, dRR, mRR, H4YR, hYR, YR, LR, mLR, zLR. dLR, meLR, AR, FR, WR, LA, dLA, mLA, LL, LY, LW, LF, WR) and argNOD (Spoof and Catherine 2017). In addition, the photodiode array spectrum was scanned for additional MCs that contained the diagnostic 232 nm/239 nm signature for MCs present in high concentration that may be missing from the above list. Method recoveries and the measurement of ion suppression were done on a subset of samples by the addition of three MCs that spanned the polarity range (RR, LR, and LF). Method recoveries and ionization efficiency were consistently greater than 90% and no correction was made for extraction efficiency or ion suppression. For many of these variants, validated reference standards do not exist, therefore the individual variants were quantified using a standard curve based on MC-LR (Abraxis Inc., Warminster, PA). This approach required the MS be tuned to give equal ionization efficiency across the polarity range of the different MCs (RR, LR, LA, and LF) and that RR be tuned to maximize the singly charged ion. Use of a single-variant standard curve similar to that used in the ELISA assay introduces about the same level of error (± 20%) when applied to the different variants. Detection limits were highly dependent on the sample volume provided (10–500 mL) and were individually calculated for each sample (median value: 0.03 μg L^{-1}; range: 0.01–4 μg L^{-1}); 85% of the samples had a method detection limit less than 0.3 μg L^{-1} total MCs, the US-EPA drinking water guideline for children, and 95% of the samples had a method detection limit less than 1.6 μg L^{-1}, the US-EPA drinking water guideline for adults (US-EPA 2015*a*). Full method details and the standard operating protocols are available (Boyer 2020).

Anatoxin-a, homoanatoxin-a, α- and β-dihydroanatoxin-a, cylindrospermopsin, epi-cylindrospermopsin, deoxycylindrospermopin, saxitoxins (PSTs), and BMAA were measured separately in the same 50% methanol extracts using tandem mass spectrometry (LC–MS/MS). Anatoxins and cylindrospermopsins were measured using a modification of EPA method 545 (US-EPA 2015*b*). BMAA was measured using a LC–MS/MS method that cleanly resolves BMAA from the isomeric compounds diamino butyrate (DAB) and amino ethyl glycine (AEG) modified from Lage et al. (2016). Saxitoxins (PSTs) including the *Lyngbya wollei* toxins were measured using HPLC-Fluorescence with post column oxidation (PCOX) (Official Methods of Analysis 2011), as this detects a wider range of cyanobacteria PST toxins than the current LC–MS/MS methods (Smith et al. 2019). Method detection limits for 90% of the samples were < 0.1 μg L^{-1}.

Quantification of chlorophyll

Chl *a* was quantified for selected sites on 26 and 28 September 2017 (Table 1). Whole-water samples were filtered onto 0.2 μm PCTE membrane filters and stored at − 20°C. Two methods were used for estimating Chl *a* concentration depending on the sampling location (Table 1). For the majority of samples, Chl *a* concentration was measured by fluorometry (TD-700, Turner Designs) following extraction in 90% (v/v) acetone at − 20°C (Welschmeyer 1994). For the remaining samples, Chl *a* concentration was determined via fluorometery (Turner 10-AU) following extraction of filtered samples in dimethylformamide (Speziale et al. 1984). Golnick et al. (2016) found that acetone extraction without filter-grinding may under-estimate Chl *a* relative to the dimethylformamide extraction method; care should be taken when comparing absolute values across methods.

Nucleic acid extraction and high-throughput sequencing

Nucleic acids were extracted from frozen samples collected on 26 September 2017 using the PowerWater

Table 1. Concentrations of Chl *a* (μg L^{-1}; mean ± SD), DIN (μmol L^{-1}; includes NH_3, NO_3, and NO_2), SRP (μmol L^{-1}), TP (μmol L^{-1}), and total MCs (μg L^{-1}, mean ± SD) via ELISA and LC–MS measured at study sites on 26 September 2017. Sites are listed in order from furthest up river (MR159) to the river mouth (MR0), and then lake sites (WB1–8). Chl *a* and total MC values are reported as means (n = 3) for all sites except where only one sample was measured. Total MC values exceeding the Ohio EPA recreation contact limit (20 μg L^{-1}) are in bold.

Region	Site	Chl *a*	MC (ELISA)	MC (LC–MS)
	MR159	1.93 ± 0.14*	0.14 ± 0.06	< MLD
	MR122	1.49 ± 0.07*	0.15 ± 0.03	< MLD
River	MR97	86.29 ± 3.62*	0.12 ± 0.06	< MLD
	MR76	79.86 ± 5.74*	0.15 ± 0.02	< MLD
	MR52	33.99 ± 20.24*	0.72 ± 0.41	< MLD
	MR15	75.58 ± 12.33*	0.64 ± 0.14	< MLD
	MR9	396†	6.5	< MLD
Estuary	MR8	—	3.4 ± 0.9	< MLD
	MR7	592†	**21**	2.31
	MR0	2951†,‡	**450**	5.09
	WB1	3.25 ± 0.72*	1.8	—
	WB2	3.95 ± 1.08*	0.69	< MLD
	WB3	2.28 ± 0.11*	0.060	< MLD
Lake	WB4	3.41 ± 0.50*	1.1	< MLD
	WB5	4.20 ± 0.28*	0.48	< MLD
	WB6	2.53 ± 0.16*	0.35	< MLD
	WB7	2.70 ± 0.33*	1.4	0.13
	WB8	3.05 ± 0.94*	1.2	0.14

MLD, minimum level of detection.
*Chlorophyll extraction method indicated as acetone.
†Chlorophyll extraction method indicated as dimethylformamide.
‡Surface scum samples indicated.

Sterivex DNA extraction kit (Qiagen) following the manufacturer's instructions. DNA quantity and quality were assessed using a NanoDrop spectrophotometer (Thermo-Fisher Scientific). Taxonomic composition of extracted DNA was assessed via amplicon sequencing of the V3-V4 hypervariable regions (341F and 785R primers, Klindworth et al. 2013) of the 16S gene using the Illumina MiSeq platform (Illumina) to generate 300-bp paired-end reads at the HudsonAlpha Institute for Biotechnology (Huntsville, AL).

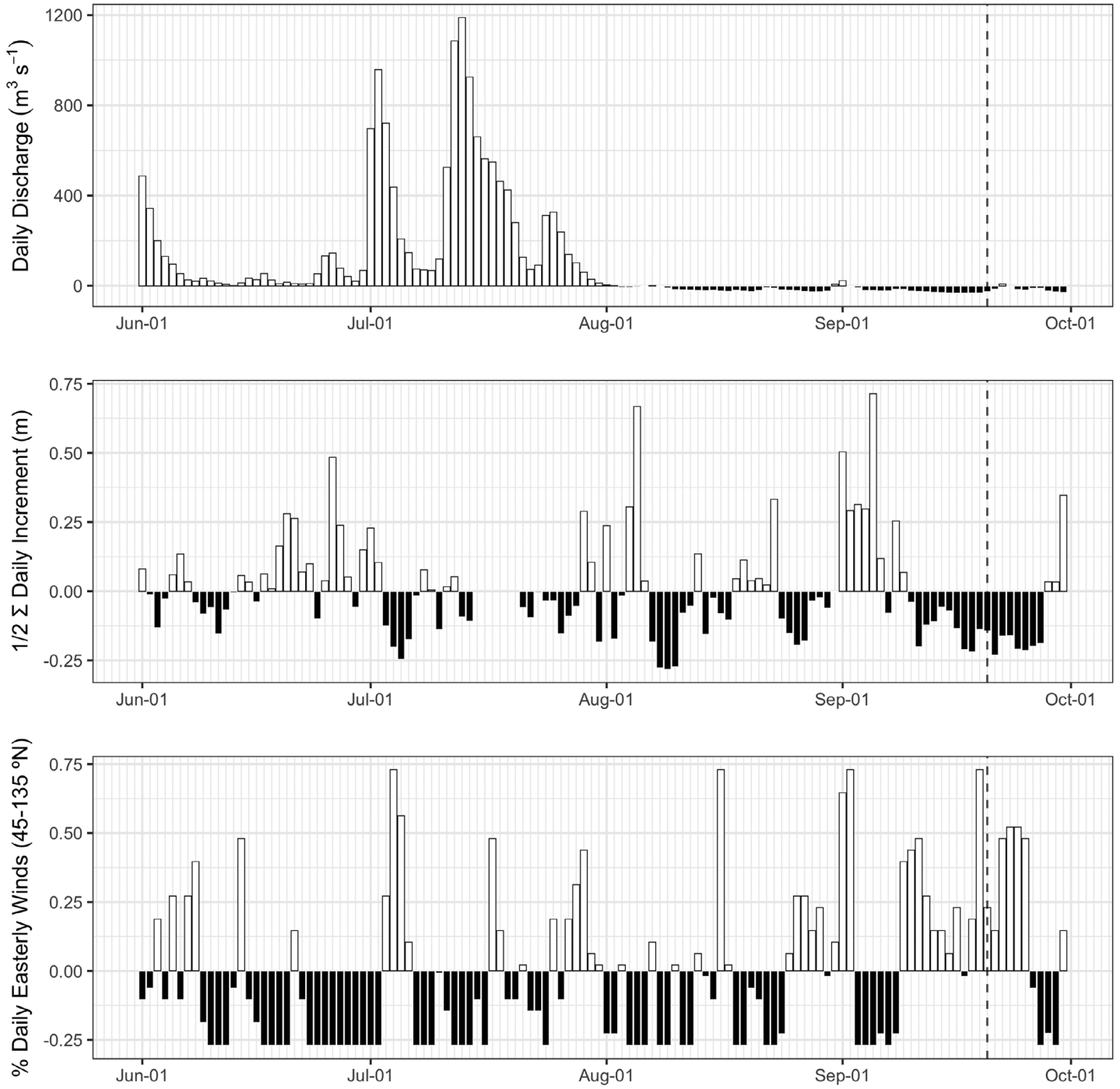

Fig. 2. Daily summer anomalies (observation minus long-term mean for June–September) for riverine discharge, seiche intensity, and easterly winds. Dashed vertical line indicates the date that bloom was first reported in the Toledo Metro area. Bar color indicates positive (white) and negative (black) anomalies.

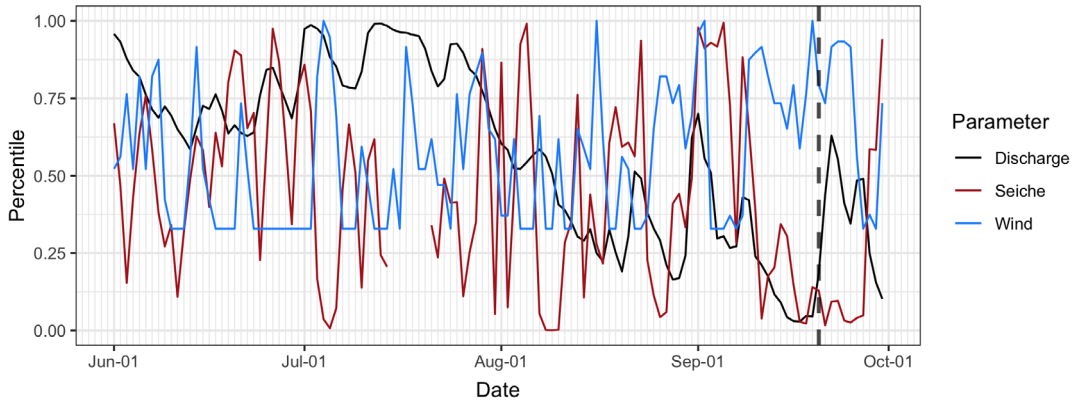

Fig. 3. Time series of 2017 observation percentiles calculated from empirical cumulative distribution functions using data from June to September for 2008–2017. Vertical dashed line represents the date that the bloom was first reported in the Toledo Metro area (20 September).

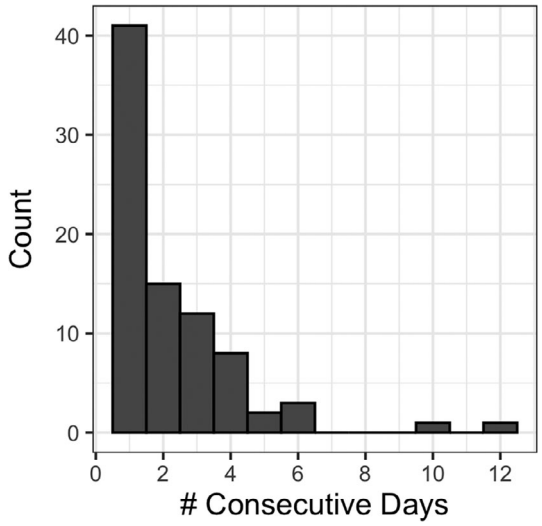

Fig. 4. Histogram showing the distribution in the length of events (# consecutive days) in which riverine discharge and seiche intensity were < 50th percentile while easterly winds were > 50th percentile during June–September from 2008 to 2017.

Bioinformatics

Demultiplexed Illumina amplicon data were processed for error correction and taxonomic assignment using the DADA2 pipeline (Callahan et al. 2016, 2017). Primers were removed (trimLeft = c[17, 21]) and reads were trimmed (270 and 220 bp for Reads 1 and 2, respectively), filtered (maxEE = c[2, 5], truncQ = 2), and denoised using the DADA algorithm. The DADA error model was parameterized for each MiSeq run using at least $1e^8$ bases. Following error correction, paired reads were merged and chimeras removed from the dataset using the consensus method. Taxonomic assignment was performed using the IDTAXA algorithm (Murali et al. 2018) with the SILVA SSU reference database (v132) training set (www2.decipher.codes/Downloads.html). Reads assigned by SILVA to eukaryote chloroplasts (Bacteria; Cyanobacteria; Oxyphotobacteria, Chloroplast) were discarded. Amplicon sequence variants (ASV) abundances were normalized by subsampling to the lowest common sequencing depth (Weiss et al. 2017); no ASVs were lost due to normalization. Data reduction filtering for representative taxa based on prevalence and abundance was conducted using Phyloseq (McMurdie and Holmes 2013). Hierarchical clustering analysis of microbial communities was performed using pvclust (Suzuki and Shimdaira 2006). Graphical visualizations were created using ggplot2 (Wickham 2016). All bioinformatic analyses and were conducted using the R Computing Framework version 3.5.1 (R Core Team 2018).

Results

Historical analysis of physical drivers of transport

Time series data for transport-related parameters (e.g., river discharge, water level, and wind direction) were analyzed from a range of observation platforms along the river and estuary to detect anomalous conditions during summer months (June through September) based on 10 years of observations from 2008 to 2017. These long-term seasonal mean values are as follows: river discharge (37.9 $m^3\ s^{-1}$; values ranged from 1.6 to 2668.6 $m^3\ s^{-1}$), seiche intensity (0.36 m; values ranged from 0.08 to 1.82 m), and the proportion of easterly winds (0.27; values ranged from 0 to 1). The episodic nature of these parameters (discharge, seiche intensity, and easterly winds) are readily apparent as anomalies during summer 2017 (Fig. 2). Above average daily discharge was primarily constrained to June and July, while daily rates of discharge after 1 August were below the seasonal mean. Seiche intensity alternated both above and below the long-term summer mean with a pronounced period of low intensity occurring from 10–27 September 2017. Seiche intensities from 8–10 Aug 2017 were the lowest during the 10-yr period. The proportion of easterly winds also exhibited temporal variability, typically oscillating over periods of days with two 8-day periods of more consistent easterly winds beginning on 8 September 2017.

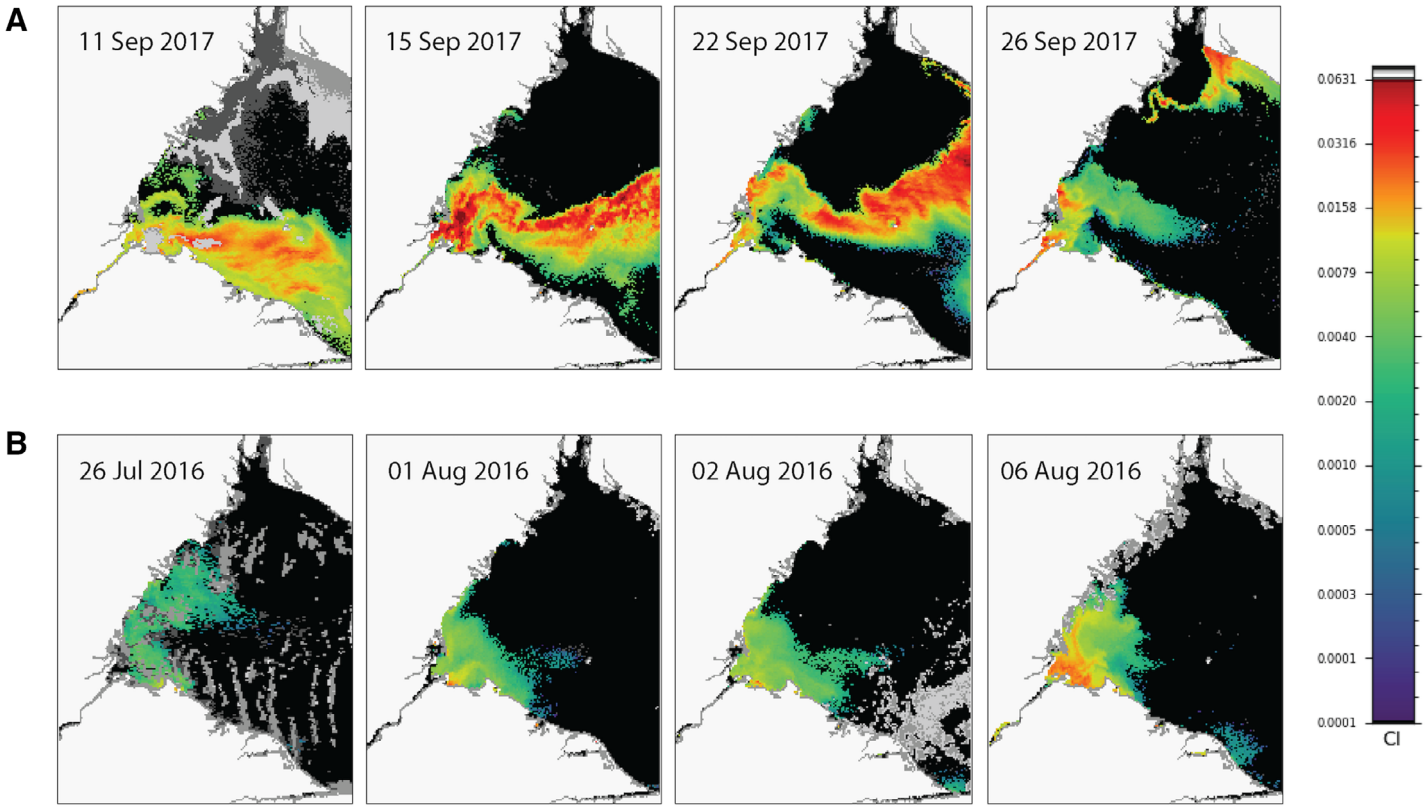

Fig. 5. Time series of daily satellite images showing the changing spatial structure of cyanobacterial blooms visualized by the cyanobacterial index (CI) in the lower Maumee River and the western basin of Lake Erie during extended high-retention periods in (**A**) 2017 and (**B**) 2016. Color scale is on the right with CI values on the left side of the bar.

A percentile-based approach was used to identify both conditions present during the bloom and their frequency during the summer over the past decade. A distinct period in which both discharge and seiche intensity were < 50th percentile while % daily easterly winds were > 50th percentile was identified preceding the bloom (Fig. 3); these concomitant conditions were identified in 190 out of 1205 total days (15.8%), ranging from 5–31 d per year. Occurring most commonly in August and September, (39.4% and 36.3%, respectively) and least in June (4.2%), these high-retention conditions were typically short events (defined as occurring ≥ 1 consecutive days), with 50% of the 84 total events lasting only 1 day, while two outlier events lasted 10 (26 July–5 August 2016) and 12 d (10–22 September 2017; Fig. 4). The longest duration event began on 10 September 2017, immediately prior to the first report of the bloom in the Toledo Metropolitan area on 20 September.

Spatial structure of blooms in river and lake for 2017 vs. 2016

Differences in the spatial structure of cyanobacterial blooms in the western basin of Lake Erie that coincided with the extended periods of high retention conditions in 2017 and 2016 were compared using satellite-based observations. During the 2017 event, an extensive CHAB was present in the region near the outset of the high-retention conditions on 11 September (Fig. 5A). During the subsequent days, the southern extension of the bloom appears to be advected to the west along the shore and cyanobacterial index (CI) values appeared to be increasing both within Maumee Bay and the Maumee River, most likely as surface scums. During the 2016 event, CI values were much weaker with a smaller distribution in this region on 26 July (Fig. 5B). A bloom appears to have developed in Maumee Bay by 6 August but did not appear to be present in the estuary, though a weak signal (< 0.0158 CI) may have been present farther up-river.

Toxin concentration and chlorophyll-estimated biomass

ELISA-based total MC values were consistently greater (5 to 27 times) than those measured by LC–MS however many of the samples were below the LC–MS detection limit. The pattern of relative concentration was similar across the study sites using both techniques (Fig. 6, Table 1). Six samples contained total MCs exceeding the State of Ohio mandated Elevated Recreational Public Health Advisory contact limit (20 μg L^{-1}, dotted line) based on ELISA, and only one exceeded this threshold based on LC–MS. Of the three dates sampled, the highest values were observed on 25 September (ranging from

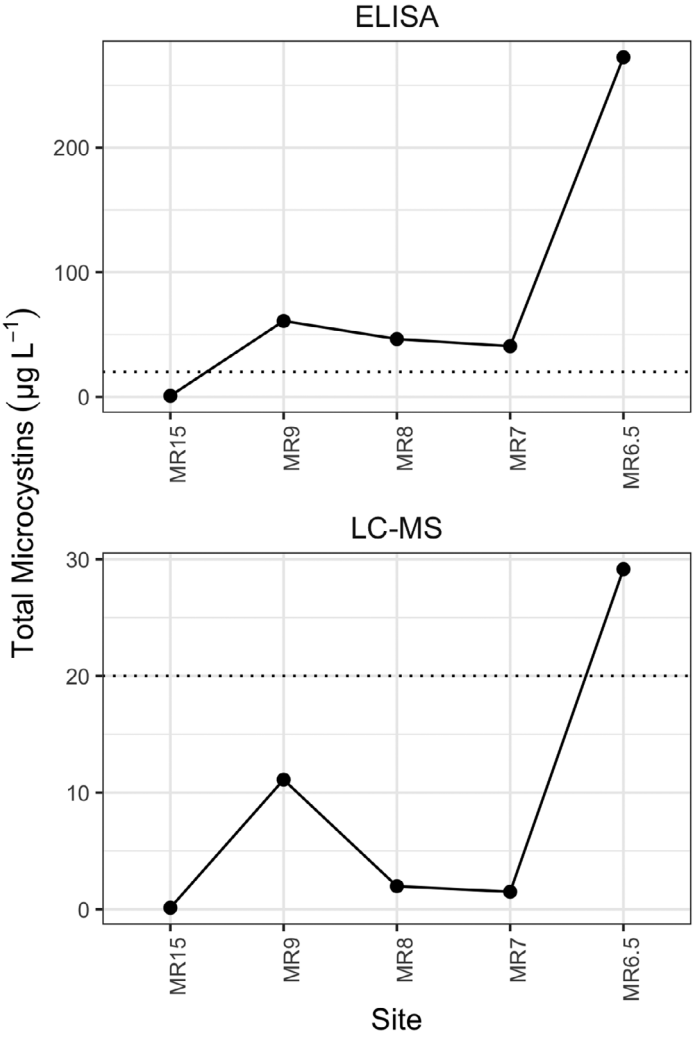

Fig. 6. Levels of total microcystins measured at estuary sites along the Maumee River on 25 September 2017 using ELISA (top row) and LC–MS (bottom row). Horizonal dashed line represents the state of Ohio elevated recreational public health advisory threshold (20 μg L^{-1}). Sites are listed in order from furthest up river within the estuary (MR15) towards the river mouth (MR6.5).

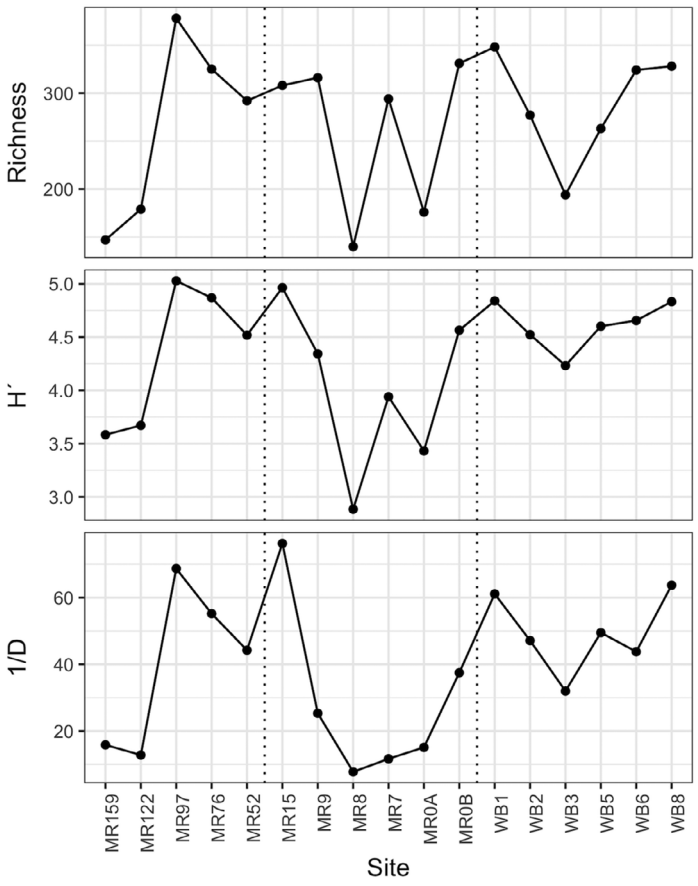

Fig. 7. Total observed number (richness), Shannon's diversity index (H′), and inverse Simpson diversity index (1/D) of 16S bacterial ASVs from sites along the Maumee River on 26 September 2017. Vertical dotted lines separate sites as river (left), estuary (middle), or lake (right). Sites are listed in order from furthest upriver (MR159) to the river mouth (MR0) and then those sampled out in Lake Erie. (**A** and **B**) Two samples were collected at MR0.

0.80 to 270 μg L^{-1} via ELISA and 0.13 to 29.15 μg L^{-1} via LC–MS; Fig. 2), potentially due to the sampling of surface scums. Sampling on 26 September covered a larger spatial range (18 sites) with ELISA values ≤ 0.72 μg L^{-1} at river and estuary sites and ≤ 0.15 μg L^{-1} at sites upriver from MR76 but increased greatly towards the river mouth, reaching 44 μg L^{-1} at MR0 (Fig. 1, Table 1). Only one site was sampled on 28 September (MR0); ELISA-based total MCs were 2.7 μg L^{-1} but below the LC–MS detection limit. Anatoxins, cylindrospermopsins, saxitoxins (PSTs), or BMAA were not detected in any samples collected during this bloom event based on LC–MS/MS or HPLC-FL analyses.

Out of the possible 22 MC variants screened for by LC–MS, only three (LR, YR, and RR) were present in these samples in concentrations above the detection limit. MC-LR was the predominate variant in all cases and was the sole variant (100%) in one-third (7 of 22) of the samples reported. However, when looking at variant profiles in low concentration samples where the total MCs are near the detection limit, the presence of minor variants may drop below the detection limit and be missed. Looking only at the samples with the highest total MC concentrations, the variant ratio was generally 2:1 MC-LR: MC-RR with variable amounts of MC-YR (0%–13%).

Chlorophyll concentrations on 26 September varied across the study sites, ranging ~ 3 orders of magnitude from 1.5 to 2951 μg L^{-1}, with chlorophyll biomass increasing towards the river mouth (Table 1, Fig. 1). An additional acetone-extracted sample was collected from MR0 on 28 September which measured 97.1 μg L^{-1}.

Taxonomic composition

Bacterioplankton community composition was determined via amplicon sequencing of the 16S rRNA gene (V3-V4 region)

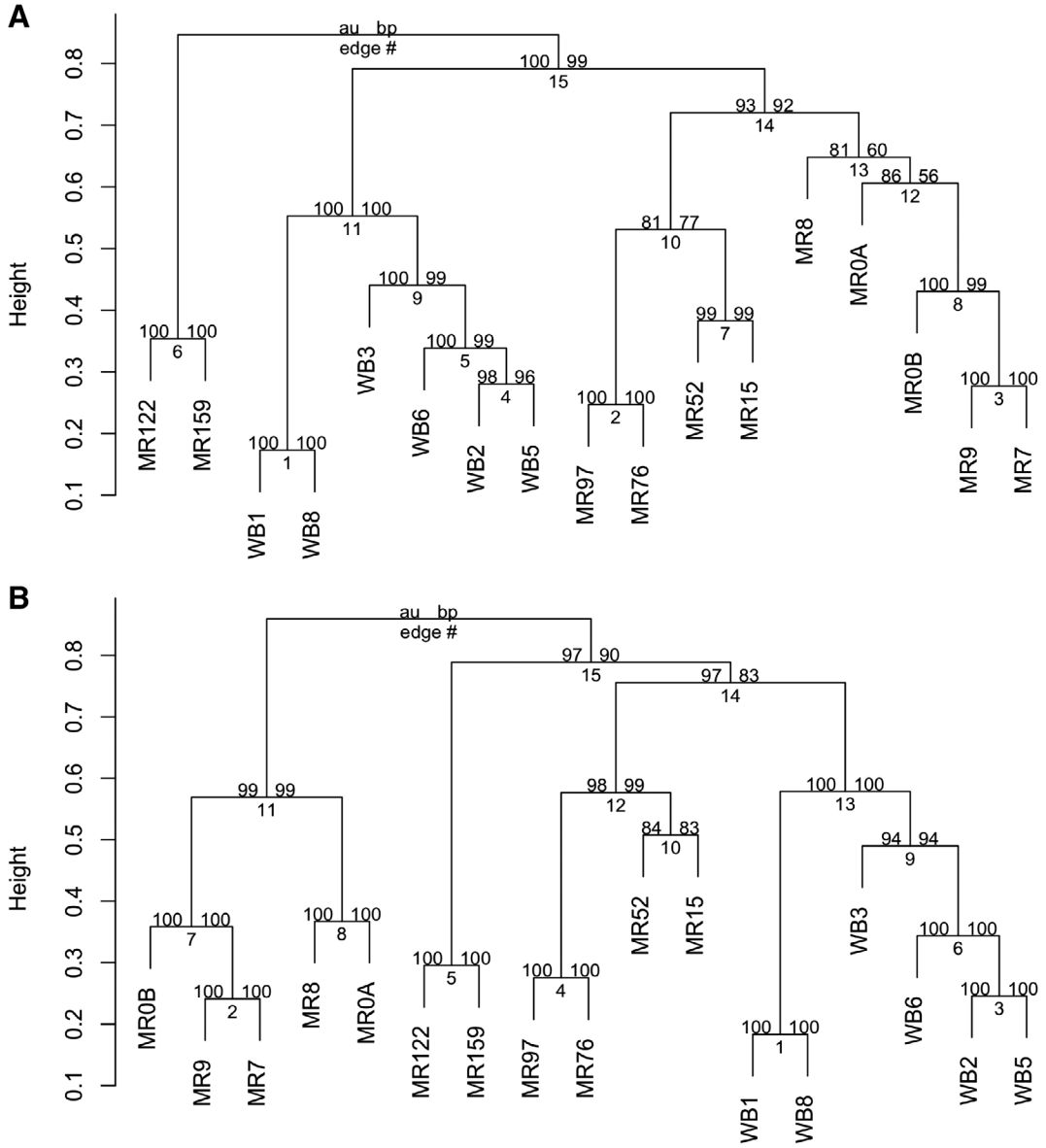

Fig. 8. Hierarchical clustering of bacterial communities sampled at study sites on 26 September using Jaccard distance (**A**) and bray–Curtis dissimilarity (**B**) matrices and average-linkage (UPGMA) clustering methods. Values above nodes reflect cluster uncertainty based on approximately unbiased *p*-values (au; left) and bootstrap probability (bp; right) generated via resampling (n = 10,000).

using samples collected along the Maumee River and in Lake Erie on 26 September 2017 (n = 17). Amplicon reads were processed using the DADA2 pipeline (Callahan et al. 2016), which allows for the identification of unique amplicon sequencing variants (ASVs). A total of 789 ASVs were detected across the 17 study sites. The observed richness of bacterial ASVs varied across the study range and within regions, ranging from 140 to 378 at each site while minimal diversity values (H´) were found within the estuary (MR8 and MR0_A). Lower values of the Inverse Simpson's Diversity Index (1/D) indicate that fewer ASVs dominate the community (e.g., MR122, MR8, and MR7) while higher values reflect a more even taxonomic composition (e.g., MR15 and MR97; Fig. 7) at a given site.

Bacterioplankton communities appeared to cluster geographically, though relationships were dependent on the dissimilarity/distance method used (Fig. 8). Based on presence/absence of ASVs (Jaccard), sites clustered into upriver (MR159 and MR122), downriver (MR97, MR76, MR52, MR15), estuary (MR9, MR8, MR7, MR0), nearshore (WB1, WB8) and open water lake communities (WB3-8) at a distance of < 0.65 with upriver having greater dissimilarity from all other sites (Fig. 8A). These clusters suggest a gradient of change in community membership at river sites approaching the estuary as

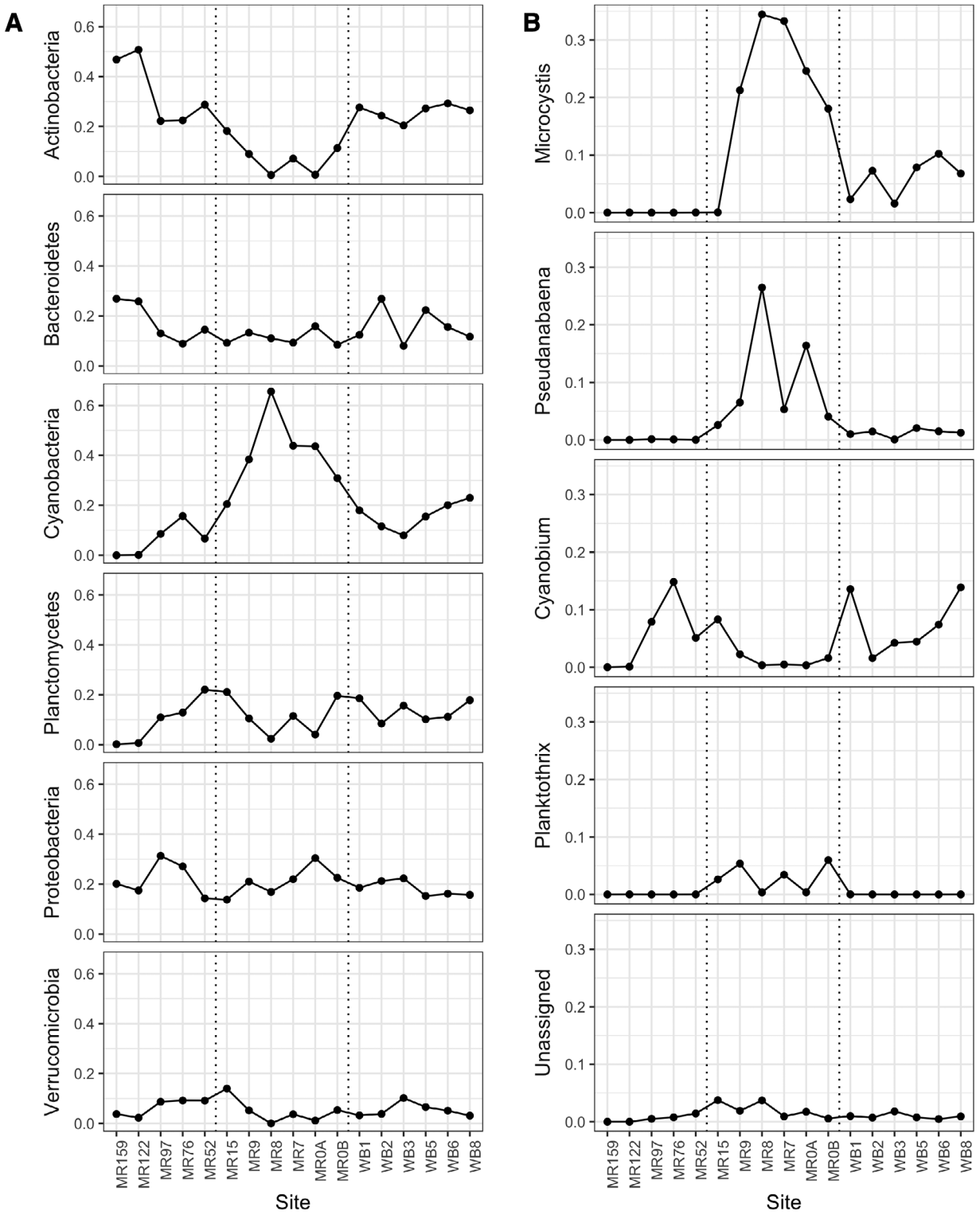

Fig. 9. Relative abundances of the (**A**) top six assigned bacterial phyla and (**B**) dominant assigned genera of cyanobacteria based on total bacterial 16S sequence reads from sites along the Maumee River on 26 September 2017. Vertical dotted lines separate sites as river (left), estuary (middle), or lake (right). (**A** and **B**) Two samples were collected at MR0.

well as between nearshore and offshore lake sites. When ASV relative abundances are taken into account (Bray-Curtis), similar clusters form at dissimilarities < 0.6 and estuarine communities (excluding MR15) showed a higher level of dissimilarity from all other sites (0.87) (Fig. 8B). Bacterioplankton communities from downriver and lake sites clustered separately from each other, with 0.76 dissimilarity overall.

The largest fluctuations in bacterial phyla between sites were found in Actinobacteria and Cyanobacteria (Fig. 9A). Actinobacteria (91 ASVs, predominantly of the hgcI clade) comprised up to 47%–51% of reads at the two farthest up-river sites (MR159 and MR122) while Cyanobacteria comprised 20%–66% of reads within estuary sites with none detected at MR159. A total of 78 cyanobacterial ASVs were identified across the study sites with four genera accounting for > 2% of total 16S reads at a given site (Fig. 9B). At the genus level within Cyanobacteria, *Microcystis* (five ASVs) comprised the highest relative abundance despite exhibiting a non-uniform distribution; it was not detected at any sites upriver from the estuary. Two of the *Microcystis* ASVs (A and B) represented 99.6% of *Microcystis* reads from the estuary sites (95% across all sites) and accounted for a maximum of 28% and 27% of the total 16S reads at a given site, respectively, with type A being most prevalent at MR8 and MR0_A while type B was most prevalent at MR9 and MR7 (Supporting Information, Fig. S1). *Pseudanabaena* (four ASVs) was detected at all but two sites (MR159 and MR122) and was the only other cyanobacterial genus to account for > 20% of the reads present at a given site (MR8), where it co-dominated with *Microcystis* (Fig. 9B). Two of the *Pseudanabaena* ASVs (A and C) accounted for 93% of *Pseudanabaena* reads from the estuary sites (94% across all sites) and accounted for up to 17% of the total 16S reads at MR8 with peak relative abundances co-occurring with *Microcystis* type A (Supporting Information, Fig. S1). The predominant cyanobacterial sequences detected at the upriver sites were assigned to the picocyanobacterium *Cyanobium* (42 ASVs), which was detected at all sites except MR159 and accounted for 14%–15% of total 16S reads at MR76 and the two nearshore lake sites (WB1 and WB8). Of the four dominant *Cyanobium* ASVs (≥ 2% total relative abundance in a sample), two were most abundant at upriver sites while the other two were most abundant at nearshore lake sites (Supporting Information, Fig. S2). *Planktothrix* (four ASVs) was only detected at low relative abundances (< 6%). The remaining ASVs were either unassigned to a genus (~ 4% maximum at a site; 11 ASVs) or were in genera with very low relative abundances (< 2% maximum at a given site; 12 ASVs).

While not included in the analyses described above, a total of 53 ASVs were assigned as chloroplast sequences by SILVA prior to removal. Queried using a plastidial 16S reference database (PhytoREF; Decelle et al. 2015), these ASVs were comprised of cryptophytes (25 ASVs), diatoms (23 ASVs), haptophytes (three ASVs), and chlorophytes (two ASVs). These chloroplast reads were in a high relative abundance (up to 30%) at upriver stations, which suggests that eukaryotic microalgae (e.g., cryptophytes, haptophytes, and diatoms) likely contributed to the chlorophyll signal observed around MR97, MR76, MR52 (Supporting Information, Fig. S2).

Discussion

Physical drivers of bloom transport

Analyses of flow-related parameters suggest that the 2017 Maumee River estuary bloom was strongly correlated with conditions supporting high-retention within the estuary. During periods of low river discharge, seiches can exert a potentially strong lake-based influence on freshwater estuaries, as evidenced by observations of current reversals up to 15 km upstream from the mouth of the Maumee River (Limnotech 2013). On the opposite end of Lake Erie, particle tracking models in the lower reach of the Buffalo River have shown the potential for seiche-driven sediment transport ≥ 5 km upstream from the mouth of the river during low discharge, high-seiche conditions (Singer et al. 2008). However, the observed seiche intensity in September 2017 was likely far too low to transport cyanobacterial cells upriver beyond the estuary. Instead, low seiche intensity indicated decreased change in water volume, thereby increasing retention in the estuary due to a lack of exchange between the river and the lake. The predominantly eastward winds likely played a more important role via the advection of surface waters (containing the positively buoyant *Microcystis* colonies which can aggregate into surface scums) into the estuary during these low-flow conditions. A general relationship has been shown using ocean observational data in which surface transport velocity of the upper 1–2 m is ~ 10% of wind velocity (U_{10}) and driven predominantly by local winds (Clarke and Van Gorder 2018). The geographic orientation of the Maumee River estuary makes it especially susceptible to wind-driven transport via easterly winds. Further, median wind speeds were 1.9 m s^{-1} from 10 to 22 September 2017, low enough to limit wind-driven mixing and maintain surface scums of *Microcystis* colonies (Cao et al. 2006; Hunter et al. 2008; Qin et al. 2018).

The historical analyses presented here suggest that high-retention conditions are not rare within the Maumee River estuary, occurring on average ~ 19 d between June and September each year over the last 10 years. This is especially true during the latter months of summer, which correspond with peak cyanobacterial abundance in western Lake Erie (Stumpf et al. 2016; Davis et al. 2019). The atypical appearance of the 2017 Maumee River bloom was likely due to the long duration of these co-occurring conditions. The majority of riverine discharge in the Maumee River occurs early in the season in conjunction with spring and early summer rainfall, with low discharge typically occurring during August and September as rainfall tends to decrease during these months (Stow et al. 2015). While observations over the past 20 years

suggests an increasing trend in high-discharge events in western Lake Erie drainages, low to moderate discharge events lack this trend with data from the Maumee River specifically displaying a negative trend (Choquette et al. 2019). However, while seasonal rainfall data for western Lake Erie typically show low accumulation leading to the aforementioned low riverine discharge during late summer/early fall, rainfall during summer 2017 was relatively low (mean cumulative daily precipitation from three airfields in the Toledo region from June 1 to Sept 30 was 9.8 cm) as compared to mean values ranging from 13.0 to 26.4 cm during the same seasonal period in the previous 3 yr (2014–2016). Therefore, the more variable components (seiche and wind direction) likely play a more prominent role in the formation and duration of high-retention conditions during this time period. Decadal shifts in summer wind direction have been previously shown in the Great Lakes region, likely driven by atmospheric variability and displacement of summer storm tracks (Waples and Klump 2002). Despite only two events lasting > 6 d over the previous 10-year period, it is possible that anthropogenic climate change could alter the frequency of these high-retention conditions in the coming years. Finally, the occurrence of high-retention conditions alone will not guarantee the formation of a bloom in the estuary. The 2017 high-retention event co-occurred with a dense cyanobacterial bloom, however a large cyanobacterial bloom was not present during the 2016 event. Climate change is expected to increase the duration, intensity, and toxin concentration of cyanobacterial blooms (O'Neil et al. 2012; Paerl and Paul 2012), leading to greater opportunities for these co-occurring conditions to occur as well as increasing the supply of propagules that could be delivered into a freshwater estuary, such as the Maumee River estuary.

Toxin concentrations

This study provides evidence that the 2017 bloom in the Maumee River estuary produced levels of cyanotoxin in excess of Ohio's Elevated Recreational Public Health Advisory contact limits. Only MCs were detected in this bloom (variants LR, YR, and RR); cylindrospermopsins, anatoxins, saxitoxins (PSTs), or free BMAA were not detected in any samples. Whereas cylindrospermopsins and anatoxins have been infrequently measured (Boyer 2007; Carmichael and Boyer 2016; Almuhtaram et al. 2018) and saxitoxin-related genes were recently detected (Chaffin et al. 2019), to date there have been no detections of BMAA in Lake Erie. The detections of total MCs exceeding Ohio's no contact thresholds (20 μg L^{-1}) were restricted to estuary sites and their magnitudes varied between analytical methods and across subsequent days. Levels of MCs observed within the estuary during the 2017 bloom (272 μg L^{-1} total MC) exceeded those observed in Lake Erie from 2012 to 2014 (maximums of 21 and 10.6 μg L^{-1} particulate MC, respectively; Gobler et al. 2016; Steffen et al. 2017) and during a bloom of *Planktothrix agardhii* that occurred upriver in the Maumee in 2016 (22.5 μg L^{-1} total MC; McKay et al. 2018). Relative proportions of the major MC variants (LR, RR, YR) were similar to those reported during the 2014 Lake Erie bloom event resulting in the Toledo Water Crisis (Steffen et al. 2017).

Greater than 250 MC variants have been identified to date (Spoof and Catherine 2017) but commercial standards were only available for a limited number of variants (14) at the time of this study. Targeted methods such as LC–MS/MS (e.g., EPA method 544) require the specific MC be available for tuning purposes and only report those variants when standards are available (US-EPA 2015*c*). As a result, these targeted methods may underreport total MCs if alternative variants are present. Samples collected during 2016 and 2017 in the western basin of Lake Erie and analyzed using LC–MS/MS were positive for seven MC variants (MC-LR, MC-RR, MC-YR, MC-LA, MC-LF, MC-LW, and linear MC-LR) with an additional 20 variants tentatively identified using high resolution mass accuracies and ADDA (Palagama et al. 2020). In contrast, nontargeted methods such as the low resolution LC–MS techniques used here or high resolution LC–MS methods (Yilmaz et al. 2019) may better quantitate total MCs by detecting a wider range of toxin variants using more generic conditions. Both targeted and nontargeted analyses may suffer from the limitation that trace levels of minor variants may fall below the detection limit. Here we used an untargeted but low-resolution technique to show that three common MC variants (LR, RR, YR) were the most common contributors to the MC profiles. Alternate non-targeted methods such as MMPB (2-methyl-3-methoxy-4-phenylbutanoic acid) integrate these minor variants/contributors to the toxin profile and may produce results more consistent with total MCs as measured by ELISA (Foss and Aubel 2015), however the MMPB method was not employed for this study.

Taxonomic composition

Identifying the cyanobacterial cells responsible for blooms and their source is important in understanding bloom dynamics. Previous studies in western Lake Erie have found evidence both for (Bridgeman et al. 2012; Conroy et al. 2014) and against (Kutovaya et al. 2012; Davis et al. 2014; Kitchens et al. 2018) fluvial seeding of cyanobacterial blooms, as well as re-suspension from sediments (Chaffin et al. 2014; Kitchens et al. 2018). Genetics-based approaches such as denaturing gradient gel electrophoresis (Chaffin et al. 2014), phylogenetic analyses (Kutovaya et al. 2012; Davis et al. 2014), and oligotyping (Berry et al. 2017*a*) allow for the biological fingerprinting of cyanobacterial strains present in different regions and bloom events.

Within the Maumee River estuary, the cyanobacterial communities were dominated by the MC-producing cyanobacterium *Microcystis*, which is commonly found within the open waters of western Lake Erie. 16S-based *Microcystis* ASVs found within the Maumee River estuary sites were also found in the

Lake Erie sites but not in river sites, which is in agreement with the advection of surface water into the estuary from the lake. The two most abundant ASVs found in the bloom are consistent with 16S oligotypes commonly found in the western basin of Lake Erie ("CCG" and "CGT" in Berry et al. 2017*a*). Two additional oligotypes ("CTT" and "TCG") identified by Berry et al. (2017*a*) were also found in this study, though in much lower relative abundances and in greater prevalence in the Lake Erie sites. Reads assigned to two other potential toxin-producing genera, *Pseudanabaena* and *Planktothrix* (Christiansen et al. 2003; Rangel et al. 2014), were also found in higher relative abundances at sites within the estuary, though less abundant than *Microcystis*. However, none of these three genera were detected at appreciable levels of relative abundance upriver from the estuary (> 20 km upriver), despite previous observations of blooms of *Microcystis* and *Planktothrix* > 96 km upstream from the mouth of the Maumee River (Bridgeman et al. 2012; Kutovaya et al. 2012; Conroy et al. 2014; McKay et al. 2018). It is interesting to note the co-occurrence of the two dominant *Pseudanabaena* ASVs with one *Microcystis* ASV (type A) but not the other, as laboratory experiments have shown the direction of *Pseudanabaena-Microcystis* interactions to be highly strain specific (Agha et al. 2016). It is likely that the *Cyanobium* ASVs identified here are equivalent to the *Synecoccocus* OTUs detected by Berry et al. (2017*b*). In an opposite pattern to Berry et al. (2017*b*), this study found the relative abundance of *Cyanobium* ASVs to be inversely related to *Microcystis* as well as in greater relative abundance at nearshore vs. offshore lake sites. Though beyond the scope of this study, potential habitat differentiation between some *Cyanobium* ASVs suggests potential utility as biological tracers for riverine inputs, as has been suggested for freshwater flows into marine environments (Mason et al. 2016).

With the exception of *Actinobacteria*, non-cyanobacterial taxa represented similar proportions of the bacterial communities across the study range. Metagenomic analyses of bacterial communities in a Spanish reservoir suggest a negative correlation between *Actinobacteria* and *Cyanobacteria* due to an inability of *Actinobacteria* to compete under bloom-favorable (warm and nutrient replete) conditions (Ghai et al. 2014). However, Berry et al. (2017*b*) found evidence for niche partitioning by Lake Erie actinobacterial OTUs in relation to the 2014 cyanobacterial bloom.

Conclusions

These results highlight the need to broaden our understanding of physical drivers that influence cyanobacterial bloom development within freshwater estuaries, which represent the interface between riverine and lacustrine systems. This is particularly important in places where these estuaries fall within large metropolitan areas, such as Toledo, OH, and other large lakes and their tributaries (Larson et al. 2013). While nutrient inputs that fuel CHABs can be reduced by modifying human activity at local and regional scales, changes in physical forcing due to climate-related factors are beyond such control and may even undermine efforts to combat CHABs through nutrient management (Ho et al. 2019). Leveraging long-term physical datasets can assist in determining the likelihood of synergistic factors occurring that may enhance cyanobacterial blooms in freshwater estuaries, improving our ability to forecast events in these habitats. This would provide opportunities for compensatory mitigation at the local and regional scales, such as by physical removal of biomass or increased water column mixing and/or flushing (Stroom and Kardinaal 2016), as well as inform decision-making strategies for geomorphological modifications of estuarine habitats, which may select for distinct and potentially toxigenic phytoplankton assemblages (Feinpeng et al. 2013). Further, phytoplankton traits play an important role in how physical drivers may influence the presence of a bloom. While buoyancy control has been shown to infer a competitive advantage for some cyanobacterial taxa (e.g., *Microcystis*, *Aphanizomenon*) to form blooms during periods of low turbulence (Carey et al. 2011), it may also allow them to concentrate biomass within the surface mixed layer thereby increasing the potential for wind-driven transport. By improving our understanding of the physical drivers (e.g., discharge, wind) and biological characteristics (e.g., –omics and toxin surveys) within these estuarine environments, we can achieve a more holistic picture of the mechanisms driving cyanobacterial harmful algal blooms in western Lake Erie and other large lakes and their tributaries.

References

Agha, R., M. del Mar Labrador, A. de los Rios, and A. Quesada. 2016. Selectivity and detrimental effects of epiphytic *Pseudanabaena* on *Microcystis* colonies. Hydrobiologia **777**: 139–148. doi:10.1007/s10750-016-2773-z

Almuhtaram, H., Y. Cui, A. Zamyadi, and R. Hofmann. 2018. Cyanotoxins and cyanobacteria cell accumulations in drinking water treatment plants with a low risk of bloom formation at the source. Toxins **10**: E430. doi:10.3390/toxins10110430

Baker, D. B., D. E. Ewing, L. T. Johnson, J. W. Kramer, B. J. Merryfield, R. B. Confesor, R. P. Richards, and A. A. Roerdink. 2014. Lagrangian analysis of the transport and processing of agricultural runoff in the lower Maumee River and Maumee Bay. J. Great Lakes Res. **40**: 479–495. doi:10.1016/j.jglr.2014.06.001

Berry, M. A., J. D. White, T. W. Davis, S. Jain, T. H. Johengen, G. J. Dick, O. Sarnelle, and V. J. Denef. 2017*a*. Are oligotypes meaningful ecological and phylogenetic units? A case study of *Microcystis* in freshwater lakes. Front. Microbiol. **8**: 365. doi:10.3389/fmicb.2017.00365

Berry, M. A., and others. 2017*b*. Cyanobacterial harmful algal blooms are a biological disturbance to Western Lake

Erie bacterial communities. Environ. Microbiol. **19**: 1149–1162. doi:10.1111/1462-2920.13640

Boyer, G. L. 2007. The occurrence of cyanobacterial toxins in New York lakes: Lessons for the MERHAB-Lower Great Lakes program. Lake Reservoir Manage. **23**: 153–160. doi:10.1080/07438140709353918

Boyer, G. L. 2020. Determination of microcystins in water samples by high performance liquid chromatography (HPLC) with single quadrupole mass spectrometry (MS). protocols.io. doi:10.17504/protocols.io.bck2iuye

Bridgeman, T. B., J. D. Chaffin, D. D. Kane, J. D. Conroy, S. E. Panek, and P. M. Armenio. 2012. From river to Lake: Phosphorus partitioning and algal community compositional changes in Western Lake Erie. J. Great Lakes Res. **38**: 90–97. doi:10.1016/j.jglr.2011.09.010

Bullerjahn, G. S., and others. 2016. Global solutions to regional problems: Collecting global expertise to address the problem of harmful algal blooms—A Lake Erie case study. Harmful Algae **54**: 223–238. doi:10.1016/j.hal.2016.01.003

Callahan, B. J., P. J. McMurdie, M. J. Rosen, A. W. Han, A. A. Johnson, and S. P. Holmes. 2016. DADA2: High-resolution sample inference from Illumina amplicon data. Nat. Methods **13**: 581–583. doi:10.1038/nmeth.3869

Callahan, B. J., P. J. McMurdie, and S. P. Holmes. 2017. Exact sequence variants should replace operational taxonomic units in marker-gene data analysis. IMSE J. **11**: 2639–2643. doi:10.1038/ismej.2017.119

Cao, H., F. Kong, L. Luo, X. Shi, Z. Yang, X. Zhang, and Y. Tao. 2006. Effects of wind and wind-induced waves on vertical phytoplankton distribution and surface blooms of *Microcystis aeruginosa* in Lake Taihu. J. Freshwater Ecol. **21**: 231–238. doi:10.1080/02705060.2006.9664991

Carey, C. C., B. W. Ibelings, E. P. Hoffmann, D. P. Hamilton, and J. D. Brooks. 2011. Eco-physiological adaptations that favour freshwater cyanobacteria in a changing climate. Water Res. **46**: 1394–1407. doi:10.1016/j.watres.2011.12.016

Carmichael, W. W., and G. L. Boyer. 2016. Health impacts from cyanobacteria harmful algae blooms: Implications for the North American Great Lakes. Harmful Algae **54**: 194–212. doi:10.1016/j.hal.2016.02.002

Chaffin, J. D., V. Sigler, and T. B. Bridgeman. 2014. Connecting the blooms: Tracking and establishing the origin of the record-breaking Lake Erie *Microcystis* bloom of 2011 using DGGE. Aquat. Microb. Ecol. **73**: 29–39. doi:10.3354/ame01708

Chaffin, J. D., and others. 2019. Cyanobacterial blooms in the central basin of Lake Erie: Potentials for cyanotoxins and environmental drivers. J. Great Lakes Res. **45**: 277–289. doi:10.1016/j.jglr.2018.12.006

Choquette, A. F., R. M. Hirsch, J. C. Murphy, L. T. Johnson, and R. B. Confesor. 2019. Tracking changes in nutrient delivery to western Lake Erie: Approaches to compensate for variability and trends in streamflow. J. Great Lakes Res. **45**: 21–39. doi:10.1016/j.jglr.2018.11.012

Christiansen G., J. Fastner, M. Erhard, T. Börner, and F. Dittmann E. 2003. Microcystin biosynthesis in *Planktothrix*: Genes, evolution, and manipulation. J. Bacteriol. **185**: 564–572. doi:10.1128/jb.185.2.564-572.2003

Clarke, A. J., and S. Van Gorder. 2018. The relationship of near-surface flow, Stokes drift, and the wind stress. J. Geophys. Res. Oceans **123**: 4680–4692. doi:10.1029/2018JC014102

Conroy, J. D., D. D. Kane, D. M. Dolan, W. J. Edwards, M. N. Charlton, and D. A. Culver. 2005. Temporal trends in Lake Erie plankton biomass: Roles of external phosphorus loading and dreissenid mussels. J. Great Lakes Res. **31**: 89–110. doi:10.1016/S0380-1330(05)70307-5

Conroy, J. D., D. D. Kane, R. D. Briland, and D. A. Culver. 2014. Systemic, early-season *Microcystis* blooms in western Lake Erie and two of its major agricultural tributaries (Maumee and Sandusky rivers). J. Great Lakes Res. **40**: 518–523. doi:10.1016/j.jglr.2014.04.015

Davis, T. W., S. B. Watson, M. J. Rozmarynowycz, J. J. H. Ciborowshi, R. M. McKay, and G. S. Bullerjahn. 2014. Phylogenies of microcystin-producing cyanobacteria in the lower Laurentiam great Lakes suggest extensive genetic connectivity. PLoS One **9**: e106093. doi:10.1371/journal.pone.0106093

Davis, T. W., and C. J. Gobler. 2016. Preface for special issue on "global expansion of harmful cyanobacterial blooms: Diversity, ecology, causes, and controls". Harmful Algae **54**: 1–3. doi:10.1016/j.hal.2016.02.003

Davis, T. W., R. Stumpf, G. S. Bullerjahn, R. M. L. McKay, J. D. Chaffin, T. B. Bridgeman, and C. Winslow. 2019. Science meets policy—A framework for determining impairment designation criteria for large waterbodies affected by cyanobacterial harmful algal blooms. Harmful Algae **81**: 59–64. doi:10.1016/j.hal.2018.11.016

Decelle, J., and others. 2015. PhytoREF: A reference database of the plastidial 16S rRNA gene of photosynthetic eukaryotes with curated taxonomy. Mol. Ecol. Resour. **15**: 1435–1445. doi:10.1111/1755-0998.12401

Palagama, D. S. W., D. Baliu-Rodriguez, B. K. Snyder, J. A. Thornburg, T. B. Bridgeman, and D. Isailovic. 2020. Identification and quantification of microcystins in western Lake Erie during 2016 and 2017 harmful algal blooms. J. Great Lakes Res. **46**: 289–301. doi:10.1016/j.jglr.2020.01.002

Esterhuizen, M., and T. G. Downey. 2008. β-N-methylamino-L-alanine (BMAA) in novel South African cyanobacterial isolates. Ecotoxicol. Environ. Saf. **71**: 309–313. doi:10.1016/j.ecoenv.2008.04.010

Feinpeng, L., Z. Haiping, Z. Yiping, X. Yihua, and C. Ling. 2013. Effect offlow velocity on phytoplankton biomass and composition in a freshwater lake. Sci. Total Environ. **447**: 64–71. doi:10.1016/j.scitotenv.2012.12.066

Foss, A. J., and M. T. Aubel. 2015. Using the MMPB technique to confirm microcystin concentrations in water measured by ELISA and HPLC (UV, MS, MS/MS). Toxicon **104**: 91–101. doi:10.1016/j.toxicon.2015.07.332

Ghai, R., C. M. Mizuno, A. Picazo, A. Camacho, and F. Rodriguez-Valera. 2014. Key roles for freshwater Actinobacteria revealed by deep metagenomic sequencing. Mol. Ecol. **23**: 6073–6090. doi:10.1111/mec.12985

Gobler, C. J., J. M. Burkholder, T. W. Davis, M. J. Harke, T. Johengen, C. S. Stow, and D. B. Van de Waal. 2016. The dual role of nitrogen supply in controlling the growth and toxicity of cyanobacterial blooms. Harmful Algae **54**: 87–97. doi:10.1016/j.hal.2016.01.010

Golnick, P. C., J. D. Chaffin, T. B. Bridgeman, B. C. Zellner, and V. E. Simons. 2016. A comparison of water sampling and analytical methods in western Lake Erie. J. Great Lakes Res. **42**: 965–971. doi:10.1016/j.jglr.2016.07.031

Herdendorf, C. E. 1970. Sand and gravel resources of the Maumee River estuary, Toledo to Perrysburg, Ohio. Ohio Division of Geological Survey. Report of Investigations 76.

Ho, J. C., A. M. Michalak, and N. Pahlevan. 2019. Widespread global increase in intense lake phytoplankton blooms since the 1980s. Nature **574**: 667–670. doi:10.1038/s41586-019-1648-7

Humbert, J. F., and others. 2013. A tribute to disorder in the genome of the bloom-forming freshwater cyanobacterium *Microcystis aeruginosa*. PLoS One **8**: e70747. doi:10.1371/journal.pone.0070747

Hunter, P. D., A. N. Tyler, N. J. Willby, and D. J. Gilvear. 2008. The spatial dynamics of vertical migration by *Microcystis aeruginosa* in a eutrophic shallow lake: A case study using high spatial resolution time-series airborne remote sensing. Limnol. Oceanogr. **53**: 2391–2406. doi:10.4319/lo.2008.53.6.2391

Kane, D. D., J. D. Conroy, R. P. Richards, D. B. Baker, and D. A. Culver. 2014. Re-eutrophication of Lake Erie: Correlations between tributary nutrient loads and phytoplankton biomass. J. Great Lakes Res. **40**: 496–501. doi:10.1016/j.jglr.2014.04.004

Kitchens, C. M., T. H. Johengen, and T. W. Davis. 2018. Establishing spatial and temporal patterns in *Microcystis* sediment seed stock viability and their relationship to subsequent bloom development in western Lake Erie. PLoS One **13**: e0206821. doi:10.1371/journal.pone.0206821

Klindworth, A., E. Pruesse, T. Schweer, J. Peplies, C. Quast, M. Horn, and F. O. Glöckner. 2013. Evaluation of general 16S ribosomal RNA gene PCR primers for classical and next-generation sequencing-based diversity studies. Nucleic Acids Res. **41**: e1. doi:10.1093/nar/gks808

Kurmayer, R., J. F. Blom, L. Deng, and J. Pernthaler. 2015. Integrating phylogeny, geographic niche partitioning and secondary metabolite synthesis in bloom-forming *Planktothrix*. ISME J. **9**: 909–921. doi:10.1038/ismej.2014.189

Kutovaya, O. A., R. M. L. McKay, B. F. N. Beall, S. W. Wilhelm, D. D. Kane, J. D. Chaffin, T. B. Bridgeman, and G. S. Bullerjahn. 2012. Evidence against fluvial seeding of recurrent toxic blooms of *Microcystis* spp. in Lake Erie's western basin. Harmful Algae **15**: 71–77. doi:10.1016/j.hal.2011.11.007

Lage, S., A. Burian, U. Rasmussen, P. R. Costa, H. Annadotter, A. Godhe, and S. Rydberg. 2016. BMAA extraction of cyanobacteria samples: Which method to choose? Environ. Sci. Pollut. Res. **23**: 338–350. doi:10.1007/s11356-015-5266-0

Larson, J. H., A. S. Trebitz, A. D. Steinman, M. J. Wiley, M. C. Mazur, V. Pebbles, H. A. Braun, and P. W. Seelbach. 2013. Great lakes rivermouth ecosystems: Scientific synthesis and management implications. J. Great Lakes Res. **39**: 513–524. doi:10.1016/j.jglr.2013.06.002

Limnotech. 2013. Development of an integrated modeling approach for quantifying the GLRI deposition metric: pilot application to Toledo Harbor; Final Technical Report prepared for U.S. Army Corps of Engineers. Buffalo District under contract to Ecology & Environment, Inc, p. 125.

Lunetta, R. S., B. A. Schaeffer, R. P. Stumpf, D. Keith, S. A. Jacobs, and M. S. Murphy. 2015. Evaluation of cyanobacteria cell count detection derived from MERIS imagery across the eastern USA. Remote Sens. Environ. **157**: 24–34. doi:10.1016/j.rse.2014.06.008

Mason, O. U., E. J. Canter, L. E. Gillies, T. K. Paisie, and B. J. Roberts. 2016. Mississippi River plume enriches microbial diversity in the northern Gulf of Mexico. Front. Microbiol. **7**: 1048. doi:10.3389/fmicb.2016.01048

McKay, R. M. L., T. Tuttle, L. A. Reitz, G. S. Bullerjahn, W. R. Cody, A. J. McDowell, and T. W. Davis. 2018. Early onset of a microcystin-producing cyanobacterial bloom in an agriculturally-influenced Great Lakes tributary. J. Oceanogr. Limnol. **36**: 1112–1125. doi:10.1007/s00343-018-7164-z

McMurdie, P. J., and S. P. Holmes. 2013. Phyloseq: An R package for reproducible interactive analysis and graphics of microbiome census data. PLoS One **8**: e61217. doi:10.1371/journal.pone.0061217

Meyer, K., T. W. Davis, S. A. Watson, M. A. Berry, V. J. Denef, and G. J. Dick. 2017. Genome sequences of lower Great Lakes *Microcystis* strains reveal strain-specific genes that are present and expressed during western Lake Erie blooms. PLoS One **12**: e0183859. doi:10.1371/journal.pone.0183859

Mitrovic, S. M., L. Hardwick, and F. Dorani. 2011. Use of flow management to mitigate cyanobacterial blooms in the lower Darling River, Australia. J. Plankton Res. **33**: 229–241. doi:10.1093/plankt/fbq094

Murali, A., A. Bhargava, and E. S. Wright. 2018. IDTAXA: A novel approach for accurate taxonomic classification of microbiome sequences. Microbiome **6**: 140. doi:10.1186/s40168-018-0521-5

Official Methods of Analysis. 2011. Method 2011.02. Gaithersburg, MD: AOAC International.

O'Neil, J. M., T. W. Davis, M. A. Burford, and C. J. Gobler. 2012. The rise of harmful cyanobacteria blooms (CHABs): The potential roles of eutrophication and climate change. Harmful Algae **14**: 313–334. doi:10.1016/j.hal.2011.10.027

Paerl, H. W., and V. J. Paul. 2012. Climate change: Links to global expansion of harmful cyanobacteria. Water Res. **46**: 1349–1363. doi:10.1016/j.watres.2011.08.002

Pearson, L., T. Mihali, M. Moffitt, R. Kellmann, and B. Neilan. 2010. On the chemistry, toxicology and genetics of the cyanobacterial toxins, microcystin, nodularin, saxitoxin and cylindrospermopsin. Mar. Drugs **8**: 1650–1680. doi:10.3390/md8051650

Qin, B., G. Yang, J. Ma, T. Wu, W. Li, L. Liu, J. Deng, and J. Zhou. 2018. Spatiotemporal changes of cyanobacterial bloom in large shallow eutrophic Lake Taihu, China. Front. Microbiol. **9**: 451. doi:10.3389/fmicb.2018.00451

R Core Team. 2018. R: A language and environment for statistical computing. Vienna, Austria: R Foundation for Statistical Computing. Available from https://www.R-project.org/.

Rangel, M., J. C. G. Martins, A. N. Garcia, G. A. A. Conserva, A. Costa-Neves, C. L. Sant'Anna, and L. R. de Carvalho. 2014. Analysis of the toxicity and histopathology induced by the oral administration of *Pseudanabaena galeata* and *Geitlerinema splendidum* (cyanobacteria) extracts to mice. Mar. Drugs **12**: 508–524. doi:10.3390/md12010508

Scheffer, M., S. Rinaldi, A. Gragnani, L. R. Mur, and E. H. van Nes. 1997. On the dominance of filamentous cyanobacteria in shallow, turbid lakes. Ecology **78**: 272–282. doi:10.2307/2265995

Singer, J., J. Atkinson, P. Manley, and P. Mclaren. 2008. Understanding sediment dynamics using geological and engineering approaches: A case study of the Buffalo River area of concern, Buffalo, New York. Intl. J. River Basin Manag. **6**: 1–10. doi:10.1080/15715124.2008.9635335

Smith, Z. J., R. M. Martin, B. Wei, S. W. Wilhelm, and G. L. Boyer. 2019. Spatial and temporal variation in paralytic shellfish toxin production by benthic *Microseira (Lyngbya) wollei* in a freshwater New York lake. Toxins (Basel) **11**: 44–62. doi:10.3390/toxins11010044

Speziale, B. J., S. P. Schreiner, P. A. Giammatteo, and J. E. Schindler. 1984. Comparison of N, N-dimethylformamide, dimethylsulfoxide, and acetone for extraction of phytoplankton chlorophyll. Can. J. Fish. Aquat. Sci. **41**: 1519–1522. doi:10.1139/f84-187

Spoof, L., and A. Catherine. 2017. Appendix 3 tables of microcystins and Nodularins, p. 526–537. *In* J. Meriluoto, L. Spoof, and G. A. Codd [eds.], Handbook of cyanobacterial monitoring and cyanotoxin analysis. Wiley. doi:10.1002/9781119068761

Steffen, M. M., and others. 2017. Ecophysiological examination of the Lake Erie *Microcystis* bloom in 2014: Linkages between biology and the water supply shutdown of Toledo, OH. Environ. Sci. Technol. **51**: 6745–6755. doi:10.1021/acs.est.7b00856

Stow, C. A., Y. Cha, L. T. Johnson, R. Confesor, and R. P. Richards. 2015. Long-term and season trend decomposition of Maumee River nutrient inputs to western Lake Erie. Environ. Sci. Technol. **49**: 3392–3400. doi:10.1021/es5062648

Stroom, J. M., and W. E. A. Kardinaal. 2016. How to combat cyanobacterial blooms: Strategy toward preventive lake restoration and reactive control measures. Aquat. Ecol. **50**: 541–576. doi:10.1007/s10452-016-9593-0

Stumpf, R. P., L. T. Johnson, T. T. Wynne, and D. B. Baker. 2016. Forecasting annual cyano- bacterial bloom biomass to inform management decisions in Lake Erie. J. Great Lakes Res. **42**: 1174–1183. doi:10.1016/j.jglr.2016.08.006

Suzuki, R., and H. Shimdaira. 2006. Pvclust: An R package for assessing the uncertainty in hierarchical clustering. Bioinformatics **22**: 1540–1542. doi:10.1093/bioinformatics/btl117

Trebitz, A. S., J. A. Morrice, and A. M. Cotter. 2002. Relative role of lake and tributary in hydrology of Lake Superior coastal wetlands. J. Great Lakes Res. **28**: 212–227. doi:10.1016/S0380-1330(02)70578-9

Trebitz, A. S. 2006. Characterizing seiche and tide-driven daily water level fluctuations affecting coastal ecosystems of the Great Lakes. J. Great Lakes Res. **32**: 102–116. doi:10.3394/0380-1330(2006)32[102:CSATDW]2.0.CO;2

US-EPA. 2015*a*. Drinking water health advisory for the cyanobacterial microcystin toxins. US EPA 820R-15100, June 15, 2015.

US-EPA. 2015*b*. Method 545: Determination of cylindrospermopsin and anatoxin-a in drinking water by liquid chromatography electrospray ionization tandem mass spectrometry (LC/ESI-MS/MS). EPA 815R-15-009.

US-EPA. 2015*c*. Method 544: Determination of microcystins and nodularin in drinking water by solid phase extraction and liquid chromatography/tandem mass (LC/MS/MS). May 21, 2015.

Waples, J. T., and J. V. Klump. 2002. Biophysical effects of a decadal shift in summer wind direction over the Laurentian Great Lakes. Geophys. Res. Lett. **29**: 1201. doi:10.1029/2001GL014564

Weiss, S., and others. 2017. Normalization and microbial differential abundance strategies depend upon data characteristics. Microbiome **5**: 27. doi:10.1186/s40168-017-0237-y

Welschmeyer, N. A. 1994. Fluorometric analysis of chlorophyll *a* in the presence of chlorophyll *b* and pheopigments. Limnol. Oceanogr. **39**: 985–1992. doi:10.4319/lo.1994.39.8.1985

Wickham, H. 2016. ggplot2: Elegant graphics for data analysis. New York: Springer-Verlag. doi:10.1007/978-0-387-98141-3

Wynne, T. T., R. P. Stumpf, M. C. Tomlinson, and J. Dyble. 2010. Characterizing a cyanobacterial bloom in western Lake Erie using satellite imagery and meteorological data. Limnol. Oceanogr. **55**: 2025–2036. doi:10.4319/lo.2010.55.5.2025

Yilmaz, M., A. J. Foss, C. O. Miles, M. Özen, N. Demir, M. Balcı, and D. G. Beach. 2019. Comprehensive multi-technique approach reveals the high diversity of microcystins in field collections and an associated isolate of *Microcystis aeruginosa* from a Turkish lake. Toxicon **167**: 87–100. doi:10.1016/j.toxicon.2019.06.006

Acknowledgments

We thank Capt. David Spangler for assistance with field collections in Lake Erie and Michelle Neudeck for assistance with DNA extractions in the laboratory. We declare no conflicts of interest. Funding for the field survey, sample analysis and data analysis was provided through the NOAA National Centers for Coastal Ocean Science (NCCOS) HAB Event Response program (HAB ER publication 26) and by funding from the NIH (1P01ES028939-01) and NSF (OCE-1840715) to the Great Lakes Center for Fresh Waters and Human Health at Bowling Green State University.

Conflict of Interest

None declared.

Submitted 26 August 2019
Revised 02 March 2020
Accepted 23 June 2020

Associate editor: Michele Burford